SUPPLEMENTARY MATERIALS

SUPPLEMENTARY METHODS

Performance of Publicly Available Adult and Infant Parcels on Neonatal Data

To demonstrate how much improvement our neonatal-specific parcellation provides compared to adult parcellations in terms of within-parcel FC homogeneity, we also evaluated our neonatal parcellation created from the primary dataset against several adult surface-based parcellations most commonly used in the neuroimaging literature [1–3], as well as 2 recently published infant parcels developed using datasets including young infants [4–6], on the 130 healthy, term neonates from the neonatal dataset which were not used in the generation of the parcellation.

The Wang parcellations were provided in the HCP standard fsLR 32k surface space by the authors. The Shen parcellation [5,6] was provided in the MNI volume space by the authors and was manually transformed to surface space using the Conte69 midthickness fsLR 32k surfaces using the Connectome Workbench command: "wb_command –volume-label-to-surface-mapping". The resulting file was dilated using "wb_command –cifti-dilate" with 10mm to remove all holes from the volume-to-surface transformation. Next, the isolated patches with a connected component size smaller than 0.1 of the average parcel size of each hemisphere were replaced with the mode of their neighboring vertices using the code from the CBIG repository: (https://github.com/ThomasYeoLab/CBIG/tree/master/utilities/matlab/parcellation/CBIG_CleanSurfaceParcellation.m). A final step removed parcels smaller than 10 vertices.

Area homogeneity of each parcel was calculated as the proportion of variance across all vertices' connectivity patterns that can be explained by the first principal component [3] and the homogeneity of the parcellation is the average of the homogeneity of all parcels within the parcellation. A homogeneity Z-score was also calculated using the mean and standard deviation of homogeneities from 1000 randomly rotated parcellations on the cortex [3] to account for the potential impact of parcel size and shape on its homogeneity. To create such randomly rotated parcellations, as in analyses in the main text, we rotated each hemisphere of the original parcellation a random amount around each of the x, y and z axes on the spherical expansion of the 32k fs_LR cortical surface. Each parcel was then slightly dilated or contracted to adjust for vertices gained or lost due to the non-uniform vertex density across the surface of the sphere, thus maintaining the same number of vertices within the rotated parcel while approximately maintain the same shape. In any random rotation, some parcels will be rotated into the medial wall (where no data exist) or into high signal dropout areas. In cases where area parcels have fewer than 15 vertices outside the high signal dropout areas (defined as regions where mean BOLD percentage change were 25% below

the mode value across all voxels on average throughout the entire scan session, i.e., mean BOLD <750 for BOLD 1000 normalized data) or the medial wall, their homogeneities were not calculated and were imputed by the average homogeneity of all random versions of the parcel in the rest of the 1000 rotations.

SUPPLEMENTARY TABLES

Neonatal Characteristics (n=131)	***n***	**Mean**	**SD**
Sex			
Male	78		
Female	53		
Gestational age at birth (weeks)		38.5	0.99
Postmenstrual age at scan (weeks)		41.2	1.2
Birthweight in grams		3267.9	466.1
Area deprivation index		69.4	24.4
Child's race			
African American	48		
White	81		
Chinese	2		
Other Pacific Islander	0		
Other	0		
Mixed African American/White	0		
Mixed Chinese/White	0		
Ethnicity			
Hispanic	3		
Non-Hispanic	128		
Neonatal fMRI Characteristics	***n***	**Mean**	**SD**
fMRI data collected (minutes)		22.8	2.7
fMRI data retained (minutes)		20.2	2.8

Supplementary Table 1: *Demographics for the primary generation dataset which the neonatal boundary map and parcels were generated from.*

Neonatal Characteristics (n=66)	***n***	**Mean**	**SD**
Sex			
Male	39		
Female	27		
Gestational age at birth (weeks)		38.5	1.0
Postmenstrual age at scan (weeks)		41.2	1.3
Birthweight in grams		3238.5	467.5
Area deprivation index		71.8	25.1
Child's race			
African American	44		
White	21		
Chinese	1		
Other Pacific Islander	0		
Other	0		
Mixed African American/White	0		
Mixed Chinese/White	0		
Ethnicity			
Hispanic	1		
Non-Hispanic	65		
Neonatal fMRI Characteristics	***n***	**Mean**	**SD**
fMRI data collected (minutes)		22.7	3.0
fMRI data retained (minutes)		20.3	3.3

Neonatal Characteristics (n=65)	***n***	**Mean**	**SD**
Sex			
Male	39		
Female	26		
Gestational age at birth (weeks)		38.5	0.97
Postmenstrual age at scan (weeks)		41.1	1.2
Birthweight in grams		3297.6	466.4
Area deprivation index		70.0	23.6
Child's race			
African American		37	
White		27	
Chinese		1	
Other Pacific Islander		0	
Other		0	
Mixed African American/White		0	
Mixed Chinese/White		0	
Ethnicity			
Hispanic		2	
Non-Hispanic		63	
Neonatal fMRI Characteristics	***n***	**Mean**	**SD**
fMRI data collected (minutes)		23.0	2.4
fMRI data retained (minutes)		20.1	2.1

Supplementary Table 2: *Demographic information for each split half of the primary dataset.*

Network Assignment Name	Number Assignment	Color Assignment	RGB Color Code			
Unassigned	0	Gray	128	128	128	
Posterior Default Mode	1	Red	255	0	0	
Anterior Default Mode	2	Watermelon	235	61	84	
Superior Precuneus	3	Hot Pink	255	26	185	
Posterior Fronto-parietal	4	Yellow	230	230	0	
Anterior Fronto-parietal	5	White	255	255	255	
Inferior Fronto-parietal	6	Cream	255	253	208	
Precentral Fronto-parietal	7	Mustard	252	194	0	
Lateral Orbito-Frontal	8	Citron	237	255	176	
Medial Orbito-Frontal	9	UCLA Blue	79	123	176	
Salience	10	Black	0	0	0	
Ventral Attention	11	Teal	0	153	153	
Cingulate	12	Toothpaste	0	255	193	
Dorsal Attention	13	Green	0	204	0	
Posterior Premotor	14	Pink	255	153	255	
Anterior Premotor	15	Forest Green	0	102	0	
Inferior Precuneus	16	Royal Blue	0	0	255	
Anterior Precuneus	17	Lime	165	255	80	
Medial Visual	18	Tan	255	179	102	
Lateral Visual	19	Dark Blue	0	0	153	
Auditory	20	Purple	153	51	255	
Insula	21	Plum	148	0	108	
Superior Motor	22	Cyan	0	255	255	
Inferior Motor	23	Orange	255	128	0	

Parcel Number	Network Assignment	Network Assignment Name	Network Assignment Color
1	1	Posterior Default Mode	Red
2	14	Posterior Premotor	Pink
3	2	Anterior Default Mode	Watermelon
4	19	Lateral Visual	Dark Blue
5	1	Posterior Default Mode	Red
6	1	Posterior Default Mode	Red
7	23	Inferior Motor	Orange
8	11	Ventral Attention	Teal
9	12	Cingulate	Toothpaste
10	18	Medial Visual	Tan

11	18	Medial Visual	Tan
12	18	Medial Visual	Tan
13	1	Posterior Default Mode	Red
14	18	Medial Visual	Tan
15	22	Superior Motor	Cyan
16	10	Salience	Black
17	10	Salience	Black
18	12	Cingulate	Toothpaste
19	12	Cingulate	Toothpaste
20	12	Cingulate	Toothpaste
21	10	Salience	Black
22	1	Posterior Default Mode	Red
23	1	Posterior Default Mode	Red
24	22	Superior Motor	Cyan
25	22	Superior Motor	Cyan
26	22	Superior Motor	Cyan
27	17	Anterior Precuneus	Lime
28	16	Inferior Precuneus	Royal Blue
29	17	Anterior Precuneus	Lime
30	23	Inferior Motor	Orange
31	23	Inferior Motor	Orange
32	13	Dorsal Attention	Green
33	2	Anterior Default Mode	Watermelon
34	2	Anterior Default Mode	Watermelon
35	22	Superior Motor	Cyan
36	22	Superior Motor	Cyan
37	15	Anterior Premotor	Forest Green
38	15	Anterior Premotor	Forest Green
39	2	Anterior Default Mode	Watermelon
40	14	Posterior Premotor	Pink
41	13	Dorsal Attention	Green
42	23	Inferior Motor	Orange
43	13	Dorsal Attention	Green
44	13	Dorsal Attention	Green
45	22	Superior Motor	Cyan
46	23	Inferior Motor	Orange
47	23	Inferior Motor	Orange
48	1	Posterior Default Mode	Red
49	11	Ventral Attention	Teal
50	20	Auditory	Purple
51	20	Auditory	Purple

52	23	Inferior Motor	Orange
53	1	Posterior Default Mode	Red
54	20	Auditory	Purple
55	20	Auditory	Purple
56	20	Auditory	Purple
57	11	Ventral Attention	Teal
58	11	Ventral Attention	Teal
59	20	Auditory	Purple
60	20	Auditory	Purple
61	20	Auditory	Purple
62	20	Auditory	Purple
63	20	Auditory	Purple
64	8	Lateral Orbito-Frontal	Citron
65	10	Salience	Black
66	21	Insula	Plum
67	6	Inferior Fronto-parietal	Cream
68	6	Inferior Fronto-parietal	Cream
69	9	Medial Orbito-Frontal	UCLA Blue
70	21	Insula	Plum
71	10	Salience	Black
72	10	Salience	Black
73	8	Lateral Orbito-Frontal	Citron
74	19	Lateral Visual	Dark Blue
75	1	Posterior Default Mode	Red
76	1	Posterior Default Mode	Red
77	18	Medial Visual	Tan
78	18	Medial Visual	Tan
79	3	Superior Precuneus	Hot Pink
80	19	Lateral Visual	Dark Blue
81	1	Posterior Default Mode	Red
82	1	Posterior Default Mode	Red
83	1	Posterior Default Mode	Red
84	19	Lateral Visual	Dark Blue
85	1	Posterior Default Mode	Red
86	19	Lateral Visual	Dark Blue
87	4	Posterior Fronto-parietal	Yellow
88	19	Lateral Visual	Dark Blue
89	19	Lateral Visual	Dark Blue
90	19	Lateral Visual	Dark Blue
91	19	Lateral Visual	Dark Blue
92	19	Lateral Visual	Dark Blue

93	19	Lateral Visual	Dark Blue
94	1	Posterior Default Mode	Red
95	23	Inferior Motor	Orange
96	23	Inferior Motor	Orange
97	13	Dorsal Attention	Green
98	7	Precentral Fronto-parietal	Mustard
99	8	Lateral Orbito-Frontal	Citron
100	10	Salience	Black
101	7	Precentral Fronto-parietal	Mustard
102	21	Insula	Plum
103	13	Dorsal Attention	Green
104	13	Dorsal Attention	Green
105	13	Dorsal Attention	Green
106	5	Anterior Fronto-parietal	White
107	2	Anterior Default Mode	Watermelon
108	9	Medial Orbito-Frontal	UCLA Blue
109	8	Lateral Orbito-Frontal	Citron
110	10	Salience	Black
111	2	Anterior Default Mode	Watermelon
112	2	Anterior Default Mode	Watermelon
113	1	Posterior Default Mode	Red
114	1	Posterior Default Mode	Red
115	11	Ventral Attention	Teal
116	18	Medial Visual	Tan
117	18	Medial Visual	Tan
118	0	Unassigned	Gray
119	18	Medial Visual	Tan
120	19	Lateral Visual	Dark Blue
121	19	Lateral Visual	Dark Blue
122	19	Lateral Visual	Dark Blue
123	19	Lateral Visual	Dark Blue
124	18	Medial Visual	Tan
125	18	Medial Visual	Tan
126	18	Medial Visual	Tan
127	18	Medial Visual	Tan
128	18	Medial Visual	Tan
129	18	Medial Visual	Tan
130	18	Medial Visual	Tan
131	18	Medial Visual	Tan
132	0	Unassigned	Gray
133	18	Medial Visual	Tan

134	5	Anterior Fronto-parietal	White
135	2	Anterior Default Mode	Watermelon
136	5	Anterior Fronto-parietal	White
137	2	Anterior Default Mode	Watermelon
138	2	Anterior Default Mode	Watermelon
139	2	Anterior Default Mode	Watermelon
140	7	Precentral Fronto-parietal	Mustard
141	7	Precentral Fronto-parietal	Mustard
142	20	Auditory	Purple
143	11	Ventral Attention	Teal
144	11	Ventral Attention	Teal
145	11	Ventral Attention	Teal
146	1	Posterior Default Mode	Red
147	1	Posterior Default Mode	Red
148	22	Superior Motor	Cyan
149	23	Inferior Motor	Orange
150	2	Anterior Default Mode	Watermelon
151	19	Lateral Visual	Dark Blue
152	1	Posterior Default Mode	Red
153	1	Posterior Default Mode	Red
154	23	Inferior Motor	Orange
155	12	Cingulate	Toothpaste
156	18	Medial Visual	Tan
157	18	Medial Visual	Tan
158	18	Medial Visual	Tan
159	18	Medial Visual	Tan
160	18	Medial Visual	Tan
161	18	Medial Visual	Tan
162	22	Superior Motor	Cyan
163	10	Salience	Black
164	10	Salience	Black
165	12	Cingulate	Toothpaste
166	12	Cingulate	Toothpaste
167	10	Salience	Black
168	1	Posterior Default Mode	Red
169	22	Superior Motor	Cyan
170	17	Anterior Precuneus	Lime
171	16	Inferior Precuneus	Royal Blue
172	17	Anterior Precuneus	Lime
173	22	Superior Motor	Cyan
174	22	Superior Motor	Cyan

175	2	Anterior Default Mode	Watermelon
176	22	Superior Motor	Cyan
177	22	Superior Motor	Cyan
178	15	Anterior Premotor	Forest Green
179	22	Superior Motor	Cyan
180	14	Posterior Premotor	Pink
181	13	Dorsal Attention	Green
182	13	Dorsal Attention	Green
183	23	Inferior Motor	Orange
184	23	Inferior Motor	Orange
185	1	Posterior Default Mode	Red
186	11	Ventral Attention	Teal
187	20	Auditory	Purple
188	20	Auditory	Purple
189	1	Posterior Default Mode	Red
190	1	Posterior Default Mode	Red
191	20	Auditory	Purple
192	11	Ventral Attention	Teal
193	11	Ventral Attention	Teal
194	20	Auditory	Purple
195	11	Ventral Attention	Teal
196	8	Lateral Orbito-Frontal	Citron
197	10	Salience	Black
198	21	Insula	Plum
199	6	Inferior Fronto-parietal	Cream
200	9	Medial Orbito-Frontal	UCLA Blue
201	10	Salience	Black
202	10	Salience	Black
203	10	Salience	Black
204	8	Lateral Orbito-Frontal	Citron
205	19	Lateral Visual	Dark Blue
206	19	Lateral Visual	Dark Blue
207	1	Posterior Default Mode	Red
208	18	Medial Visual	Tan
209	18	Medial Visual	Tan
210	3	Superior Precuneus	Hot Pink
211	1	Posterior Default Mode	Red
212	1	Posterior Default Mode	Red
213	19	Lateral Visual	Dark Blue
214	4	Posterior Fronto-parietal	Yellow
215	19	Lateral Visual	Dark Blue

216	19	Lateral Visual	Dark Blue
217	19	Lateral Visual	Dark Blue
218	1	Posterior Default Mode	Red
219	1	Posterior Default Mode	Red
220	23	Inferior Motor	Orange
221	23	Inferior Motor	Orange
222	23	Inferior Motor	Orange
223	13	Dorsal Attention	Green
224	23	Inferior Motor	Orange
225	13	Dorsal Attention	Green
226	7	Precentral Fronto-parietal	Mustard
227	7	Precentral Fronto-parietal	Mustard
228	21	Insula	Plum
229	13	Dorsal Attention	Green
230	13	Dorsal Attention	Green
231	13	Dorsal Attention	Green
232	5	Anterior Fronto-parietal	White
233	2	Anterior Default Mode	Watermelon
234	9	Medial Orbito-Frontal	UCLA Blue
235	8	Lateral Orbito-Frontal	Citron
236	5	Anterior Fronto-parietal	White
237	10	Salience	Black
238	10	Salience	Black
239	2	Anterior Default Mode	Watermelon
240	2	Anterior Default Mode	Watermelon
241	2	Anterior Default Mode	Watermelon
242	1	Posterior Default Mode	Red
243	1	Posterior Default Mode	Red
244	11	Ventral Attention	Teal
245	18	Medial Visual	Tan
246	18	Medial Visual	Tan
247	18	Medial Visual	Tan
248	0	Unassigned	Gray
249	18	Medial Visual	Tan
250	19	Lateral Visual	Dark Blue
251	19	Lateral Visual	Dark Blue
252	19	Lateral Visual	Dark Blue
253	19	Lateral Visual	Dark Blue
254	18	Medial Visual	Tan
255	18	Medial Visual	Tan
256	18	Medial Visual	Tan

257	18	Medial Visual	Tan
258	18	Medial Visual	Tan
259	18	Medial Visual	Tan
260	18	Medial Visual	Tan
261	18	Medial Visual	Tan
262	18	Medial Visual	Tan
263	18	Medial Visual	Tan
264	18	Medial Visual	Tan
265	18	Medial Visual	Tan
266	0	Unassigned	Gray
267	18	Medial Visual	Tan
268	2	Anterior Default Mode	Watermelon
269	5	Anterior Fronto-parietal	White
270	2	Anterior Default Mode	Watermelon
271	5	Anterior Fronto-parietal	White
272	2	Anterior Default Mode	Watermelon
273	5	Anterior Fronto-parietal	White
274	2	Anterior Default Mode	Watermelon
275	2	Anterior Default Mode	Watermelon
276	2	Anterior Default Mode	Watermelon
277	5	Anterior Fronto-parietal	White
278	5	Anterior Fronto-parietal	White
279	2	Anterior Default Mode	Watermelon
280	2	Anterior Default Mode	Watermelon
281	20	Auditory	Purple
282	11	Ventral Attention	Teal
283	11	Ventral Attention	Teal

Supplementary Table 3: *Network identity table for each parcel.* The top table includes the name of each functional network with its corresponding network number, color, and RBG color codes. In the bottom table, each row contains information about a single parcel's network identity (network number, name, and color).

SUPPLEMENTARY FIGURES

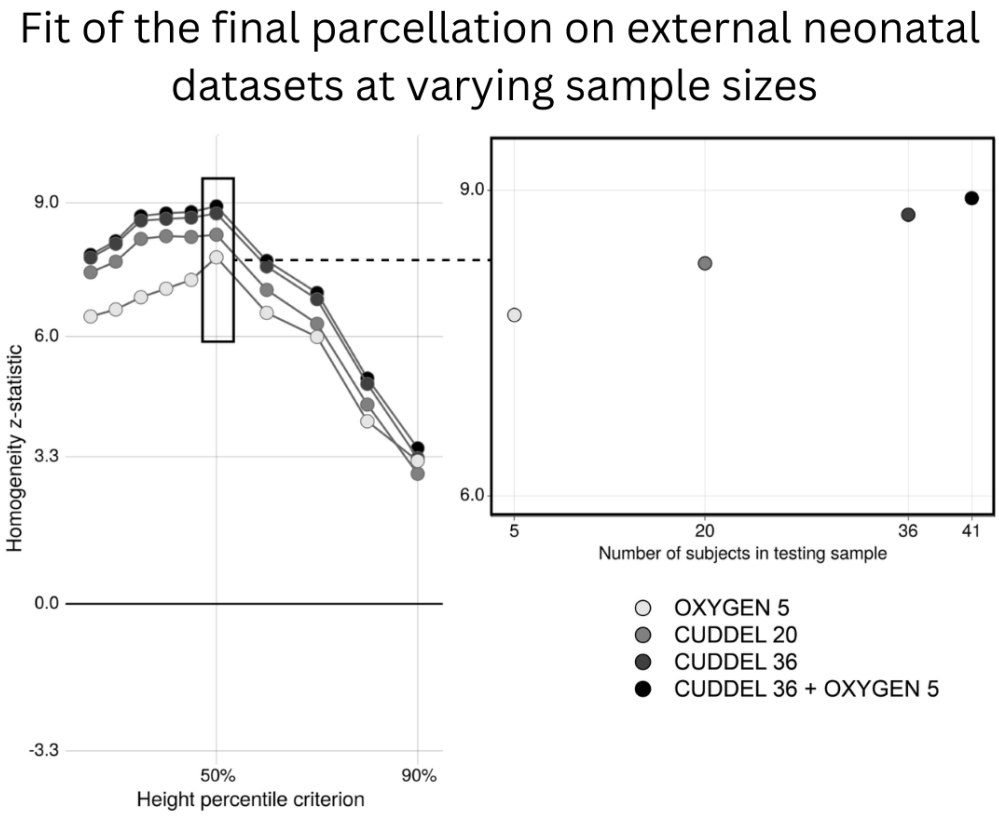

Supplementary Figure 1: *Parcellation homogeneity remained robust even with small sample sizes in external validation datasets, CUDDEL and OXYGEN.* **Left:** Homogeneity z-statistic of parcellations generated using the primary dataset (n=131) at different height percentiles tested using data from two external datasets, CUDDEL and OXYGEN. **Right**: Homogeneity z-statistic for the final parcellation (parcels from the 50% height threshold) plotted as a function of sample size for external validation datasets. Color of the dot represents the dataset and the number of subjects included in the analyses.

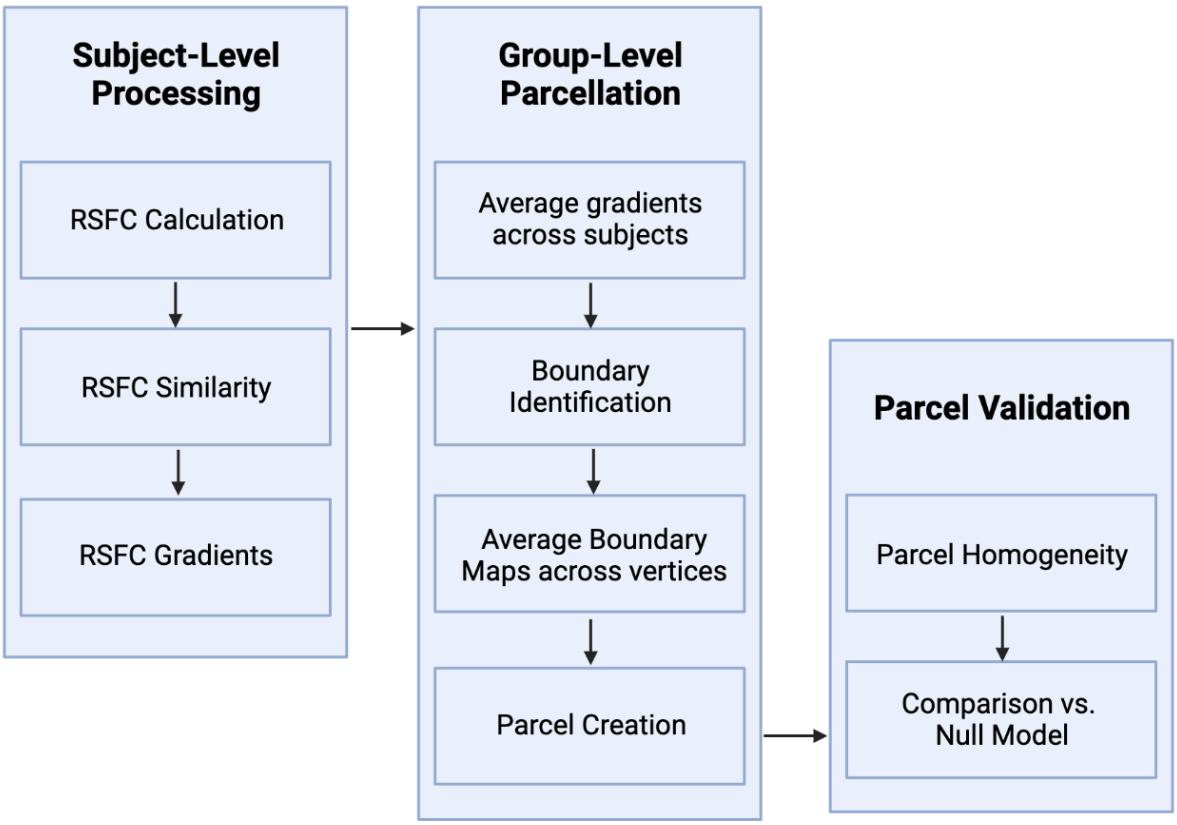

Supplementary Figure 2: *Flow of parcellation generation and validation methods.*

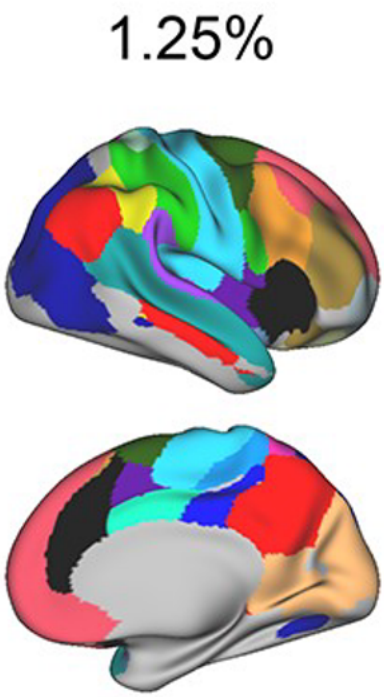

Supplementary Figure 3: *Previously described neonate-specific vertex-wise networks from Sylvester et al., 2022 used as a template for generating the consensus network assignments for the generated parcellation.* The network assignments as adapted from Figure 3A from Sylvester et al., 2022 were generated using the standard Infomap approach at the 1.25% edge density[7].

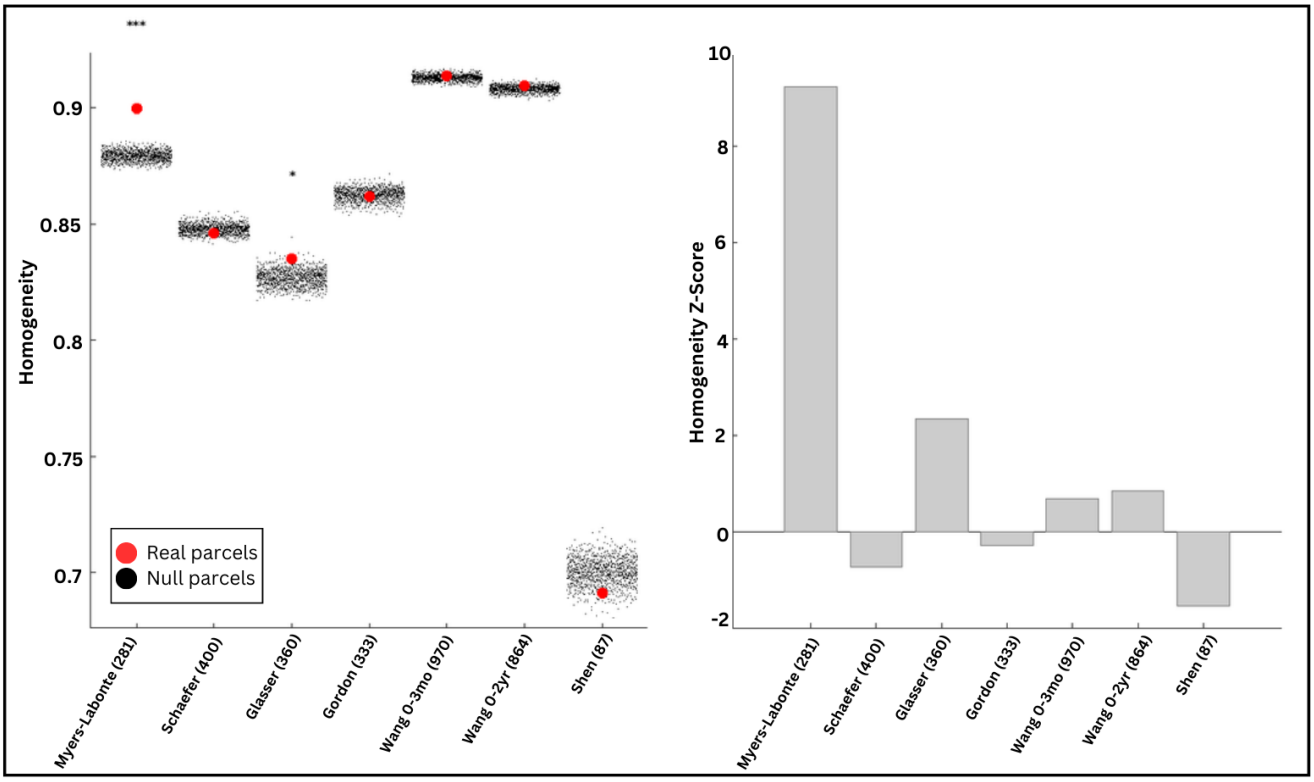

Supplementary Figure 4: *Publicly available adult parcellations perform poorly on neonatal data.* Parcellations tested include the Schaefer [2], Glasser [1], and Gordon [3] adult parcellations as well as the Wang [4] and Shen [6] parcellations from older infants. The Myers-Labonte parcellation is the parcellation from the current study. The left panel indicates true averaged homogeneity values of each parcellation tested against neonatal data (red dots) as well as null model homogeneity values for each parcellation generated by rotating the parcellation to random locations on the cortical surface (black dots). The right panel indicates homogeneity z-scores of each parcellation tested against neonatal data. The Glasser parcellation was the only parcellation to perform better than chance in the neonatal data, and its z-score (2.3) was much lower than the z-score of the parcellation generated from neonates in the current study (9.2). Note that the Myers-Labonte parcellation in the current dataset was tested against held-out data not used to generate the parcellation. Parenthetical numbers next to each parcellation name indicate the number of parcels in that parcellation.

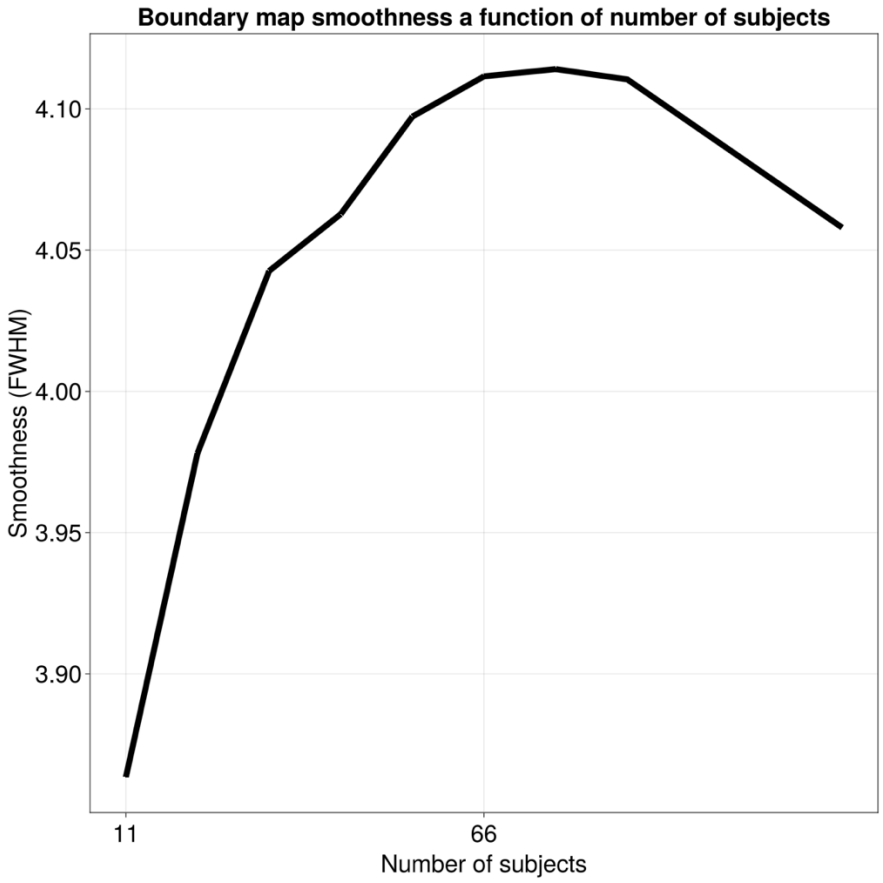

Supplementary Figure 5: *Smoothness of the neonatal boundary map increased with increasing number of subjects included in creating the average.*

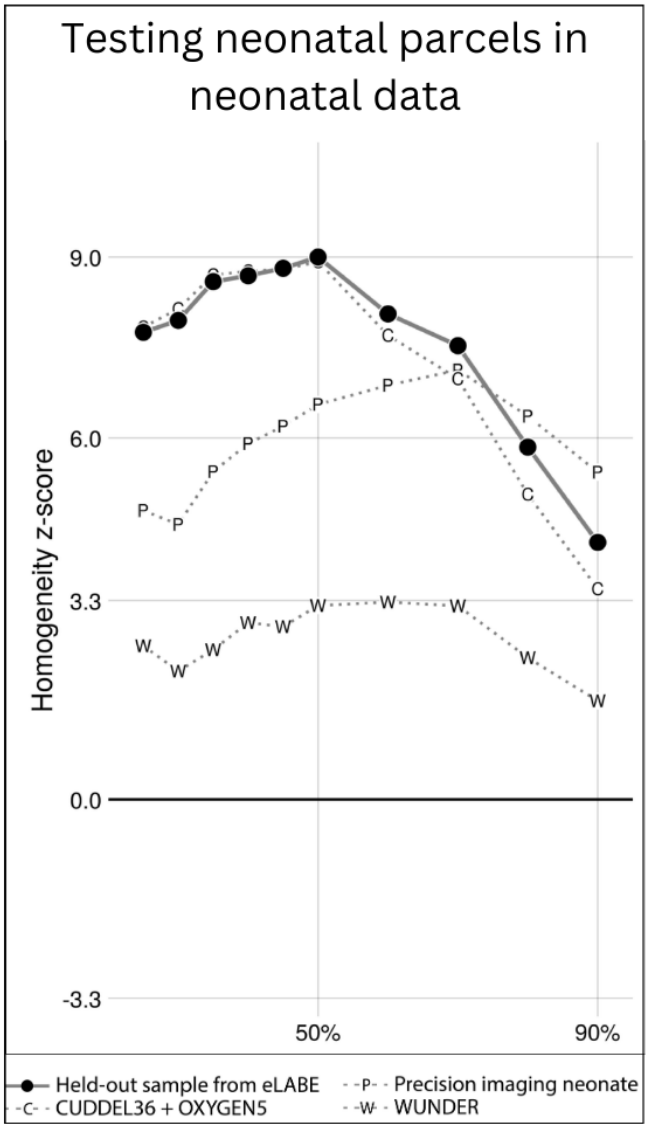

Supplementary Figure 6: *Validation of neonatal parcellations.* The primary dataset (n=131) was used to generate parcellations at varying height thresholds between 25% and 90%, which were tested in four datasets. The curves represent the homogeneity z-statistic of the parcellation generated from the primary dataset against the held-out second half of the dataset (n=130; black dots), and three external datasets (CUDDEL+OXYGEN, C; Precision Baby, PB; WUNDER, W). Note that in all cases, parcellations at 50% edge density and lower performed very well when tested against internal and external datasets.

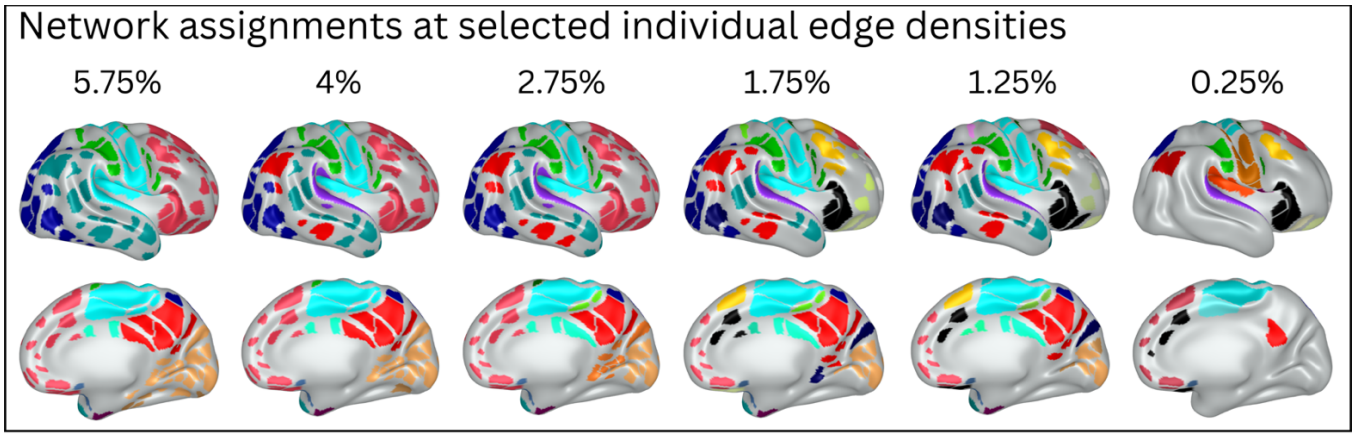

Supplementary Figure 7: *Assigned network identities at selected individual edge densities from 0.25% to 5.75%.*

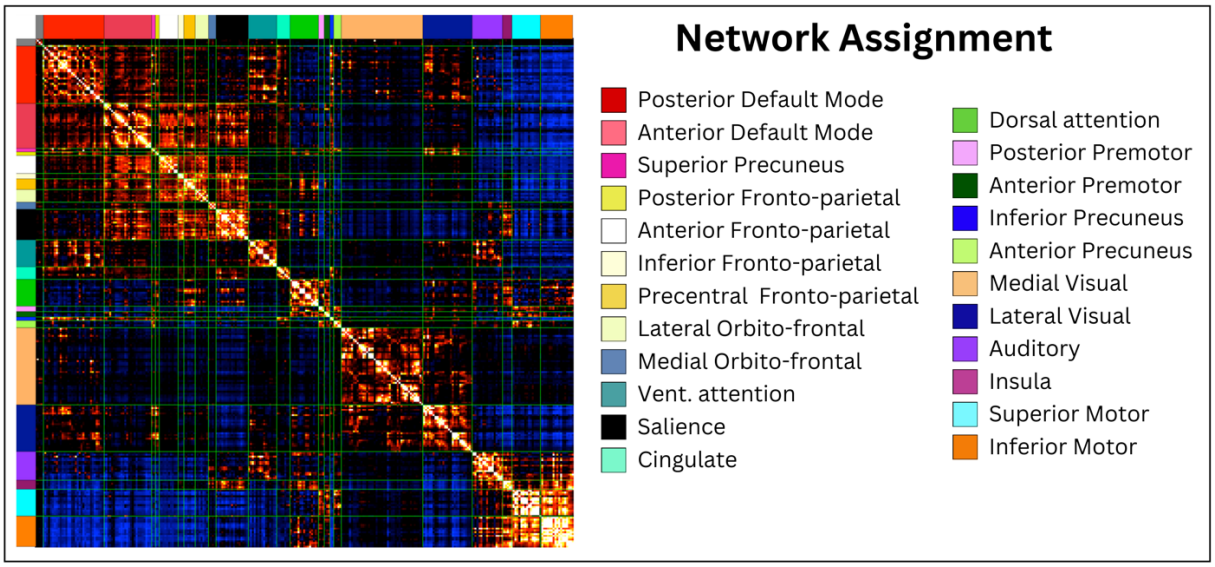

Supplementary Figure 8: *Functional connectivity matrix of the generated parcellation with parcels ordered by network identity from the consensus map.*

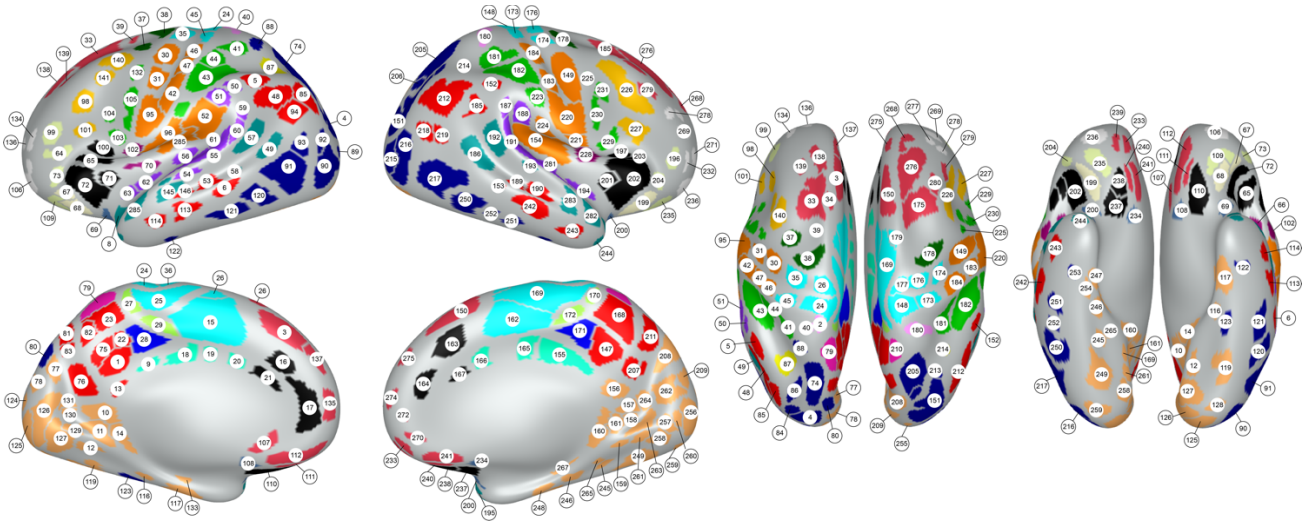

Supplementary Figure 9: *Parcels labeled with their respective parcel number and network assignment.*

SUPPLEMENTARY REFERENCES

1. Glasser, M. F. *et al.* A multi-modal parcellation of human cerebral cortex. *Nature* **536**, 171–178 (2016).
2. Schaefer, A. *et al.* Local-Global Parcellation of the Human Cerebral Cortex from Intrinsic Functional Connectivity MRI. *Cereb. Cortex* **28**, 3095–3114 (2018).
3. Gordon, E. M. *et al.* Generation and Evaluation of a Cortical Area Parcellation from Resting-State Correlations. *Cereb. Cortex* **26**, 288–303 (2016).
4. Wang, F. *et al.* Fine-grained functional parcellation maps of the infant cerebral cortex. *Elife* **12**, (2023).
5. Scheinost, D. *et al.* Preterm birth alters neonatal, functional rich club organization. *Brain Struct. Funct.* **221**, 3211–3222 (2016).
6. Shen, X., Tokoglu, F., Papademetris, X. & Constable, R. T. Groupwise whole-brain parcellation from resting-state fMRI data for network node identification. *Neuroimage* **82**, 403–415 (2013).
7. Sylvester, C. M. *et al.* Network-specific selectivity of functional connections in the neonatal brain. *Cereb. Cortex* **33**, 2200–2214 (2022).